Numerical Evaluation of Exposure to the Electromagnetic Fields of an Electronic Article Surveillance System with Postured Infant Model

Congsheng Li
College of Computer and Communication Engineering,
University of Science and Technology Beijing
Beijing 100084, China
congshengli@gmail.com

Tongning Wu
China Academy of Telecommunication Research of
Ministry of Industry and Information Technology
Beijing 100191, China
toniwoo@gmail.com

***Abstract*— This paper presents the dosimetric evaluation of the infant's exposure to electromagnetic fields from an electronic article surveillance system working at 125 kHz. A recently developed realistic infant anatomical model is deformed to achieve the standing, sitting and the supine postures. We perform the quasi-static calculation for the 99th percentile induced electric field, the peak specific absorption rate averaging over 10 g tissue and the maximum induced current density. A comparison has been made with the adult. The results show that the postures and the effective exposed part are very important factors for the dose results. The infant is not always overexposed compared with the adult. The magnetic field acquired by two methods can not be used for guidelines compliance evaluation.**

Keywords—electronic article surveillance; infant model; numerical evaluation;electromagnetic fields

I. INTRODUCTION

Realistic human anatomical models are widely used in the numerical evaluation of the exposure to electromagnetic fields (EMF). Classified by the individual age representation, the majority of the available models are for the adults [1-8] and for the children [8-10]. Infants (from several weeks to 2-year-old) can experience rapid anatomical and physical growth. But the realistic infant models are rarely reported. Down-scale the adult or the child models [11-12] to obtain an infant model can not represent their special characteristics [14].

Besides, the characteristics of the infants have produced many special exposure scenarios. For example, the infant can sit or sleep in the crib when passing the electronic article surveillance (EAS) system. These particular features are not observed in the adults or the bigger children. Hence, the dosimetric variability due to these typical postures should be evaluated.

Most of the available studies for the minors' exposure to the EAS systems focus on the frequencies of 13.56 MHz [15-17] or UHF [18]. EAS systems operating at 125 kHz are frequently used for anti-theft purposes. For the frequency band from 100 kHz to 10 MHz, the ICNIRP guidelines [19-20] prescribes three basic restrictions as the induced current density inside the body (J), the specific absorption rate (SAR) and the spatial averaging 99th percentile value of the internal electric field (E_{99}). The reference levels are E field strength (E), magnetic field strength (H) and magnetic flux density (B). But the compliance procedure for the non-uniform exposure has not yet been decided. It is essential to discuss the compliance of the evaluation.

In this paper, we assess numerically the dosimetric results of the infants' exposure to the EMF generating from the EAS systems. The studied frequency is 125 kHz. A realistic infant model is reconstructed by magnetic resonance scan [21]. We deform the models to achieve a sitting posture. The standing and the supine postures are considered as well. A realistic exposure source is modeled. The induced electric field distribution in the infant body is calculated by quasi-static approximation. The dosimetric comparison has been made with the Chinese adult male model (CM) [6]. The results show that the postures and the effective exposed part are influential to the results. The H field acquired by two popular methods can not be used for guidelines compliance evaluation.

II. POSTURED REALISTIC INFANT ANATOMICAL MODEL

A. *Infant Anatomical Model*

A male one-year-old whole body infant model is created based on the magnetic resonance scan. The model has 28 different tissues with spatial resolution of 1x1x1 mm^3. Figure 1 displays the reconstructed infant model.

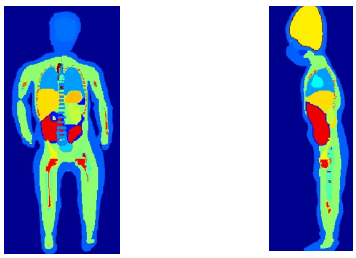

Fig. 1. Slice view of the infant model

This work was supported by the grants from National Key Basic Research Project (2011CB503705) and National Natural Science Foundation of China (Grant No. 61371187 and 61201066).

B. *Morphing Method*

The infants have three typical postures, standing (walking), supine and sitting (in the baby carriage), when passing through the EAS system. It is in significant contrast to the adults who have normally only one posture (walking or standing) when passing the EAS gate. Therefore, it is necessary to assess the dosimetric difference by various postures.

The sitting posture is deformed with the method described in Ref.12 and Ref.13. We previously compared the dosimetric variability for the standing and the supine posture (considering the displacement of the internal organs and the change of the physical profile) [23]. The result of Ref.24 shows that the displacement of the organs and the variation of the profiles due to the standing and the supine postures have insignificant effect on the internal field distribution. So, we just rotate the orientation of the model to emulate the supine posture. The three postured infant models are shown in Figure 2.

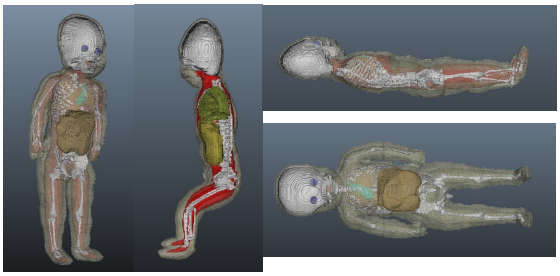

Standing **Sitting** **Supine**

Fig. 2. Postured infant model

III. Exposure Scenarios

The schema of the EAS system is obtained from Ref.15. The CAD model is shown in Figure 3. The current loop in the centre of the antenna enhances the magnetic field in this area, which can be seen in the same figure.

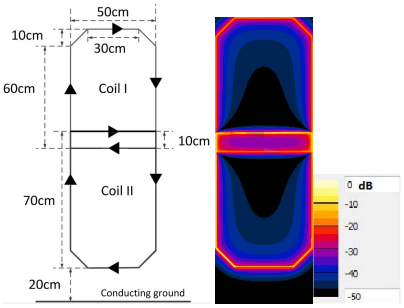

Fig. 3. Schema of the EAS antenna and the simulated magnetic field

For the supine and the sitting posture, the head of the infant is aligned to the centre loop part of the EAS antenna. For the standing posture, the feet of the infant are contacting the ground. Figure 4 shows these exposure scenarios.

The CM model with standing posture [23] is utilized in the simulation for comparison.

20 cm is kept between the antenna and the models' right armpit (both the infant and the adult model).

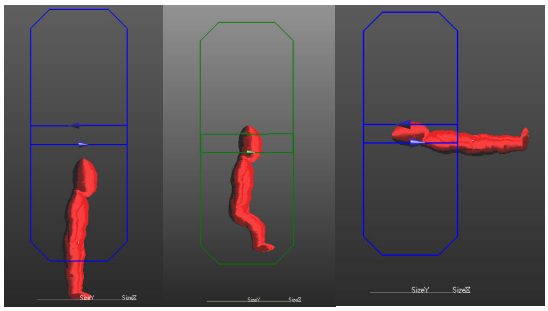

Standing **Sitting** **Supine**

Fig. 4. Simulated exposure scenarios for the postured infant models

IV. Numerical Methods

The exposure at 125 KHz can be analyzed by quasi-static approximation [25]. Scalar potential finite element (SPFE) is applied to calculate the induced E field in the infant's body. The cubic element is 2 x 2 x 2 mm^3.

The solvers are implemented by SEMCAD X14.8 (http://www.speag.com/products/semcad). The calculated induced electric fields are vectorially averaged in a contiguous tissue volume of 2 x 2 x 2 mm^3 to achieve the E_{99}. The SAR averaging over tissues' mass of 10 g (SAR_{10g}) and the maximum J are computed as well.

To discuss the compliance evaluation for this highly non-uniform exposure case, we, (1) calculate the H according to EN 50357-2001 [26] and (2) average the H over the entire volume occupied by the human body as prescribed by ICNIRP guidelines 2010. Specifically, EN 50357-2001 uses the measurement grids for an adult of 1.75 m in height. Considering the physical differences of the infant, we also tailor the grid configuration surrounding the infant, as shown in Figure 5 and Table I.

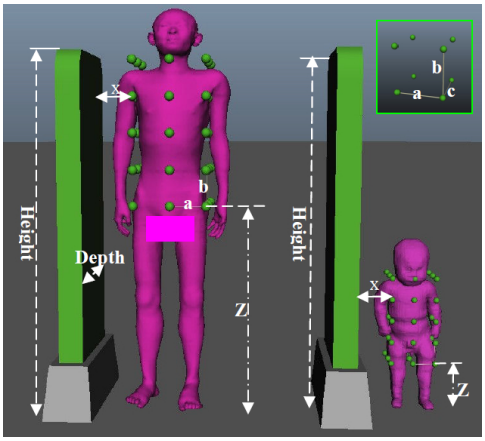

Fig. 5. The grid configurations for the H field strength

TABLE I. Grid Configurations

	a/b/c	X	Z	Height	Depth
Adult grid	15	20	85	120-160	40-80
Infant grid	8.35	20	24.80	120-160	40-80

V. RESULTS

C. Spatial average H field strength

The H field values for the various kinds of the grid configurations are list in Table II. The driven currents of 4 A and 40 A are simulated in the study (both are RMS values).

TABLE II. H VALUES FROM DIFFERENT METHODS

	EN 50357 (adult grids)	Infant grids	Whole body average			
			CM	Infant		
			Standing	*Standing*	*Sitting*	*Supine*
Average RMS |H| (A/m)	1.61/ 16.08	1.72/ 17.20	0.14/ 1.43	0.03/ 0.33	0.04/ 0.38	0.02/ 0.21
Maximum RMS |H| (A/m)	3.51/ 35.08	2.52/ 25.22	5.83/ 58.25	3.22/ 32.23	3.55/ 35.53	4.55/ 45.52

The format of the data is: (4 A current / 40 A current)

D. Dosimetric results for the postured infant models and the CM model

The peak SAR_{10g}, the E_{99} and the maximum J for the CM and the infant model with three postures are shown in Table III, Table IV, Figure 6 and Figure 7. We provide the results by driven currents of 4 A and 40 A (RMS values).

TABLE III. PEAK SAR_{10g} RESULTS

		Infant			CM
		Standing	*Sitting*	*Supine*	*Standing*
peak SAR_{10g} (W/kg)	**4 A**	1.67e-6	2.28e-6	1.79e-6	8.82e-6
	40 A	1.66e-4	2.28e-4	1.79e-4	8.82e-4

TABLE IV. E_{99} RESULTS

		Infant			CM
		Standing	*Sitting*	*Supine*	*standing*
E_{99} **(CNS) V/m**	**4 A**	0.061	0.075	0.073	0.056
	40 A	0.61	0.75	0.75	0.56
E_{99} **(Whole body) V/m**	**4 A**	0.11	0.14	0.13	0.20
	40 A	1.12	1.38	1.29	2.00

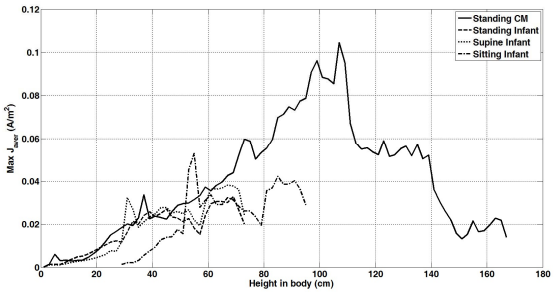

Fig. 6. Maximum J for the CM and the infant models with three postures (4 A RMS)

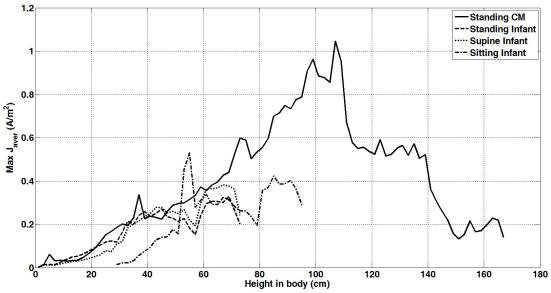

Fig. 7. Maximum J for the CM and the infant models with three postures (40 A RMS)

VI. DISCUSSIONS

A. Inter-posture analysis for the infant model

The studied three postures of the infant model can substantially vary the dosimetric results. For the standing postures, the head of the infant is below the centre loop (where the H field is enhanced), whist the head of the supine and the sitting postures are aligned to the centre loop. Hence, the resulting peak SAR_{10g}, E_{99} and max. J are lower for the latter two postures. It reveals that the variation is mainly due to the highly non-uniform field and the effective exposed body part.

B. Dosimetric comparison for the standing postures

When we compare the dosimetric results for the standing CM and the infant model, inconsistency is observed. That is, the peak SAR_{10g} for the adult is 5 time higher than that of the infant, while the E_{99} is very similar for the two cases. To investigate the reason, we calculate the 100th percentile E value (peak) in the cube of 2 x 2 x 2 mm^3. The ratio of peak E between the standing adult and the infant is about 7 times which is consistent with the ratio of the peak SAR_{10g}. So, we believe that the reason for the inconsistency is that peak SAR_{10g} is a much strict metric than E_{99}. It is reported that the 100th percentile E value contains the staircasing error. Further analysis will be conduct to reduce this error [28].

The results also show that the dose in the infant is not necessarily higher than that in the adult. The result is also consistent with the previous report on 10 MHz [29].

C. Discussion on the compliance evaluation

We augment the driven current for 10 times, the H field values acquired by the two approaches (mean value over the grids and the mean value in the volume occupied by the body) increased for 10 times. The peak SAR_{10g} increases 100 times. E_{99} and the max. J are raised for 10 times. It demonstrates that for the fixed model, there exists a good linear correlation for the external field and the internal dose.

However, higher H field values (by the two approaches) do not introduce higher internal dose for different models. Further

work needs to be done for evaluating the guidelines compliance in this kind of non-uniform exposure scenario.

VII. CONCLUSION

We numerically evaluate the exposure to the EAS system (125 kHz) with a realistic infant model and an adult model. The typical postures of the infant can influence significantly the internal dose. The adult is not necessarily underexposed compared with the infant. It reveals that the exposure to this kind of non-uniform EMF is so complicated that the posture, the realistic source and the effective exposed part should be taken into consideration. H field results obtained by two different approaches can not be associated with the peak SAR_{10g} , E_{99} and the max. J. The guidelines compliance procedure for this kind of system need to be studied.

REFERENCES

[1] M.J. Ackerman, "Accessing the Visible Human Project," D-Lib Magazine. 1995, 1(4), available from http://www.nlm.nih.gov/research/visible/visible_human.html.

[2] P.J.Dimbylow, "The development of realistic voxel phantoms for electromagnetic field dosimetry," Proc Int. Workshop on Voxel Phantom Development (National Radiological Protection Board Report). 1996, pp. 1-7.

[3] P.J. Dimbylow, "Development of the female voxel phantom, NAOMI, and its application to calculations of induced current densities and electric fields from applied low frequency magnetic and electric fields," Phys. Med. Biol. 2005, vol. 50(6), pp. 1047.

[4] C.H. Kim, S.H. Choi, J.H. Jeong, C. Lee, and M.S. Chung, "HDRK-man: a whole body voxel model based on high resolution color slice images of a Korean adult male cadaver," Phys. Med. Biol. 2008, 53(15), pp. 4093.

[5] I.G. Zubal, C.R. Harrell, E.O. Smith, and A.L. Smith, "Two dedicated voxel-based anthropomorphic (torso and head) phantoms," Proc. of the Int. Conf. at the National Radiological Protection Board. 1995, pp. 105-111.

[6] T.N. Wu, L. Tan, Q. Shao, C. Zhang, C. Zhao, Y. Li, et al. "Chinese adult anatomical models and the application in evaluation of RF exposures," Physics in medicine and biology. 2011, 56(7), pp. 2075.

[7] A.K. Lee, W.Y. Choi, M.S. Chung, H.D. Choi, and J.I. Choi, "Development of Korean Male Body Model for Computational Dosimetry," ETRI Journal. 2006, 28(1), pp. 107-110.

[8] A. Christ, W. Kainz, E.G. Hahn, K. Honegger, M. Zefferer, E. Neufeld, et al. "The Virtual Family—development of surface-based anatomical models of two adults and two children for dosimetric simulations," Phys. Med. Biol. 2010, 55(2), pp. 23-38.

[9] A.K. Lee, J.K. Byun, J.S. Park, H.D. Choi, and J. Yun, "Development of 7-year-old Korean child model for computational dosimetry," ETRI J. 2009, 31(2), pp. 237-239.

[10] G. Williams, M. Zankl, W. Abmayr, R. Veit, and G. Drexler, "The calculations of dose from external photon exposures using reference and realistic human phantoms and Monte Carlo methods," Physics in medicine and biology. 1986, 31(4), pp. 449.

[11] T. Nagaoka, E. Kunieda, and S. Watanabe, "Proportion-corrected scaled voxel models for Japanese children and their application to the numerical dosimetry of specific absorption rate for frequencies from 30 MHz to 3 GHz," Phys Med Biol. 2008, 53(23), pp. 6695-6671.

[12] A. Hadjem, D. Lautru, C. Dale, M.F. Wong, V.F. Hanna, and J. Wiart, "Comparison of specific absorption rate (SAR) induced in child-sized and adult heads using a dual band mobile phone," IEEE MTT-S Int. Microwave Symp Dig 3. 2004, pp. 1453-1456.

[13] C. Li, Q. Chen, Y. Xie and T. Wu, "Dosimetric study on eye's exposure to wide band radio frequency electromagnetic fields: Variability by the ocular axial length". Bioelectromagnetics 2014, Early View. doi: 10.1002/bem.21835.

[14] D.F. Huelke, "An Overview of Anatomical Considerations of Infants and Children in the Adult World of Automobile Safety Design," Annu Proc Assoc Adv Automot Med. 1998, 42, pp. 93-133.

[15] M. Martinéz-Búrdalo, A. Sanchis, A. Martin, and R. Villar, "Comparison of SAR and induced current densities in adults and children exposed to electromagnetic fields from electronic article surveillance devices," Physics in medicine and biology. 2010, 55(4), pp. 1041.

[16] J.F. Bakker, M.M.Paulides, A. Christ, N. Kuster, and G.C. Van Rhoon, "Assessment of induced SAR in children exposed to electromagnetic plane waves between 10 MHz and 5.6 GHz," Physics in medicine and biology. 2010, 55(11), pp. 3115.

[17] S. Fiocchi, I.A. Markakis, P. Ravazzani, and T. Samaras, "SAR Exposure From UHF RFID Reader in Adult, Child, Pregnant Woman, and Fetus Anatomical Models," Bioelectromagnetics. 2013, 34(6), pp. 443–452.

[18] S. Fiocchi, M. Parazzini, A. Paglialonga, and P. Ravazzani, "Computational exposure assessment of electromagnetic fields generated by an RFID system for mother–newborn identity reconfirmation," Bioelectromagnetics. 2011, 32(5), pp. 408-416.

[19] ICNIRP (International Commission on Non-ionizing Radiation Protection) 1998 Guidelines for limiting exposure to time-varying electric, magnetic and electromagnetic field (up to 300GHz) Healthy Phys. 74 494-522.

[20] ICNIRP, "Guidelines for limiting exposure to time-varying electric and magnetic fields (1 Hz to 100 kHz)," Health Phys. 2010, 99, pp. 818-836.

[21] C. Li , Z. Chen, L. Yang, B. Lv, J. Liu, N. Varsier, et al "Generation of infant anatomical models for evaluating the electromagnetic fields exposure," Accepted by Bioelectromagnetics, 2014.

[22] T. Nagaoka, and S. Watanabe, "Voxel-based variable posture models of human anatomy," Proceedings of the IEEE. 2009, 97(12), pp. 2015-2025.

[23] T.N. Wu, L. Tan, Q. Shao, Y. Li, L. Yang, C. Zhao, et al. "Slice-based supine-to-standing posture deformation for Chinese anatomical models and the dosimetric results with wide band frequency electromagnetic field exposure: morphing," Radiation protection dosimetry. 2013, 154(1), pp. 26-30.

[24] T.N. Wu, L. Tan, Q. Shao, Y. Li, L. Yang, C. Zhao, et al. "Slice-based supine-to-standing posture deformation for Chinese anatomical models and the dosimetric results with wide band frequency electromagnetic field exposure: simulation," Radiation protection dosimetry. 2013, 154(1), pp. 31-36.

[25] A. Hirata, F. Ito, and I. Laakso, "Confirmation of quasi-static approximation in SAR evaluation for a wireless power transfer system," Physics in medicine and biology. 2013, 58(17), N241.

[26] CENELEC (European Committee for Electrotechnical Standardization) "Evaluation of human exposure to electromagnetic fields from devices used in Electronic Article Surveillance (EAS), Radio Frequency identification (RFID) and similar applications," 2001, EN50357, pp. 1–53.

[27] W. Joseph, L.Verloock, G. Vermeeren, F.Goeminne, and L. Martens, "Assessment of field exposure by electronic article surveillance systems," BEMS, Halifax, 2011.

[28] I. Laakso, A Hirata, "Reducing the staircasing error in computational dosimetry of low-frequency electromagnetic fields," Physics in medicine and biology, 2012, 57(4), N25.

[29] M.Martinéz-Búrdalo, A. Sanchis, A. Martin, and R.Villar, "Comparison of SAR and induced current densities in adults and children exposed to electromagnetic fields from electronic article surveillance devices,". Physics in medicine and biology, 2012, 55(4), 1041.